Development of a novel method to prepare Fe- and Al-doped titanium dioxide (TiO_2) from wastewater

H.K. Shon[1], H.J. Park[2], S. Vigneswaran[1], D.L. Cho[2],
J.B. Kim[3], G.J. Kim[4] and J.-H. Kim[2,3,*]

[1] Faculty of Engineering, University of Technology, Sydney, P.O. Box 123, Broadway, NSW 2007, Australia

[2] School of Applied Chemical Engineering & Center for Functional Nano Fine Chemicals (BK21), Chonnam National University, Gwangju 500-757, Korea

[3] Photo & Environmental Technology Co. Ltd., Gwangju 500-460, Korea

[4] Department of Chemical Engineering, 253 Yonghyun-dong, Nam-gu, Inha University, Incheon, 402-751, Korea

[*] The author to whom all the correspondence should be addressed.
Email: jonghkim@chonnam.ac.kr

ABSTRCT

A simple and novel method to synthesize iron and aluminium-doped titanium dioxide (TiO_2) was investigated. Titanium tetrachloride ($TiCl_4$) was used as a coagulant to remove organic matter from wastewater. The settled floc (sludge) was dewatered and incinerated at 600 ˚C after $TiCl_4$ flocculation. The resultant by-product from the waste sludge was valuable TiO_2. $TiCl_4$ coagulant was added with $FeCl_3$ and $Al_2(SO_4)_3$ coagulants to dope iron and aluminium on TiO_2 in a flocculation process. The effect of iron and aluminium on TiO_2 was investigated in terms of scanning electron microscopy/ energy dispersive X-ray (SEM/EDX), X-ray diffraction (XRD), optical absorbance and photocatalytic activity. The majority of Fe/ and Al/TiO_2 particles were found to be less than 1 μm size formed by 0.1 μm agglomerates using SEM analysis. Fe/TiO_2 included Ti, O, C, P and Fe elements and Al/TiO_2 consisted of Ti, O, C, P and Al elements as confirmed by EDX results. Remaining organic carbon from the settled organic matter was the source of C atom in TiO_2 whereas the P atom in TiO_2 came from phosphorus nutrient present in wastewater. As iron concentration increased, the atomic percentage of the iron element in Fe/TiO_2 increased significantly from 0.27 at% (low iron concentration) to 9.83 at% (high iron concentration). However, the atomic percentage of the Al element in Al/TiO_2 increased slightly from 0.1 at% (low aluminium concentration) to 0.46 at% (high aluminium concentration) with an increase in aluminium concentration. The Fe/TiO_2 exhibited the majority of anatase phase. At higher iron concentration, hematite (Fe_2O_3) was found. The Al/TiO_2 showed anatase phase only at different aluminium concentrations. The majority of acetaldehyde with Fe/ and Al/TiO_2 was significantly removed under UV irradiation within 60 minutes. However, at higher iron concentration, acetaldehyde removal decreased by almost 50%. Under visible light irradiation, the photo-decomposition of acetaldehyde using the Fe/ and Al/TiO_2 was marginal.

Keywords: Titanium oxide, iron doping, aluminium doping, wastewater, flocculation

INTRODUCTION

Sludge disposal is one of the major problems in wastewater treatment plants. Chemical treatment by flocculation produces a large amount of sludge (settled floc) and this is generally disposed in landfill – a solution which is becoming less acceptable in view of the growing community resistance to finding new disposal sites or expanding existing ones. Treatment methods for efficient sludge recycling are therefore needed.

A novel flocculation system for producing functional TiO_2 using wastewater was investigated to reduce a large amount of sludge [1]. Titanium tetrachloride ($TiCl_4$) was used instead of most commonly used salts of iron ($FeCl_3$) and aluminium ($Al_2(SO_4)_3$) as an alternative coagulant to remove particulate and dissolved organic matter from wastewater in sewage treatment plants (STPs). Titanium tetrachloride ($TiCl_4$) successfully removed organic matter at the same level as Fe and Al salts. Ti sludge settled faster which made the subsequent separation process easy. After flocculation with titanium salt, the settled floc was incinerated to produce functional titanium dioxide (TiO_2) which resembled to commercial TiO_2. Thus, the use of Ti salt was more efficient than using Fe or Al salts and recovered a by-product of functional TiO_2 of 446.5 kg/day from a medium size STP of 25 mega liters per day. Ti salt costs are fairly cheap similar to Al and Fe salts. This process is efficient, economical and produces a viable commercial product not only in terms of removal of organic matter, but also in sludge reduction and wastewater reuse. The amount of TiO_2 recovered from this process fulfills the demand of TiO_2 as required in TiO_2 photo-catalysis during environmental

applications by photo-catalysis and hydrogen generation by photocatalytic water-splitting.

TiO_2 is the most widely used metal oxide for environmental applications, cosmetics, paints, electronic paper, and solar cells [2-4]. Current research has sought to improve the photo-catalytic properties of TiO_2 with metals or oxides [5-8]. Transition metals (Fe, Al, Ni, Cr, Co, W and V), metal oxides (Fe_2O_3), Cr_2O_3, CoO_2, MgO + CaO and SiO_2), transition metal ceramics (WO_3, MoO_3, Nb_2O_5, SnO_2 and ZnO) and anionic compounds (C, N and S) have been used to coat and dope TiO_2 to improve its applicability [9]. Among them, transitional metal and rare earth metal ions have been widely tried as dopants to improve the photocatalytic efficiency of TiO_2. As metal ions are doped into TiO_2, impurity energy levels in the band gap are formed. This leads to alteration of electron hole recombination. Transitional metals are either deposited or doped on the TiO_2 surfaces as metallic nanoparticles or the metals are doped as ionic dopants. A common method consists of doping in TiO_2 with transition metal cations while maintaining a good control of the primary particle size to achieve nanoscale configurations of the catalysts. The doping elements have usually been Fe, Al, Cr, V, Nb, Sb, Sn, P, and Si [10].

Iron has been used to dope TiO_2 and its photocatalytic activity was superior than the commercial Degussa P-25 under visible light irradiation [11]. Teoh et al. [12] also reported that Fe-doped TiO_2 was found to have very high photocatalytic activity under visible light irradiation than Degussa P-25. Fe^{3+} cations acted as shallow traps in the TiO_2 lattice. Optimum photocatalytic properties were achieved upon doping at a

relatively weak level. This was closely related to the dynamics of the recombination process which was linked to the distance between dopant cations in the TiO_2 lattice [13]. Fe ions trapped not only electrons but also holes, which leads to increase of photoactivity [14]. The maximum photoactivity appreared with 0.5 wt% of Fe^{3+} due to decrease in the density of the surface active centers [15]. The added Fe atoms dissolved in TiO_2 phase was found to have a rutile structure with average grain size less than 10 nm. Fe-doped powder had a higher absorption threshold in the range of 427-496 nm than the commercial P-25 powder (406 nm). The colour changed from white to bright yellow in Fe-doped powder. When Fe content exceeded 4.6 wt%, the optical property of Fe/TiO_2 absorbed visible light.

Aluminium doping has been used on TiO_2 for a potential application in thermal shock due to its stable thermal expansion coefficient and physical property [16]. Al_2O_3 and Al_2TiO_5 were observed at $AlCl_3/TiCl_4$ ratios higher than 1.1 at 1400 ºC [17]. They discovered a formation of new structure connected with Al-O-Ti framework. For Al/TiO_2, the anatase structure was stable after calcination at 800 ºC, while pure TiO_2 was easily transferred to the rutile phase after calcination above 700 ºC. The optical property of Al/TiO_2 prepared by a thermal plasma method responded visible light [18]. They also found that the size of synthesized powder decreased with increase in the amount of Al because Al species inhibited the particle growth. Al/TiO_2 has been applied to gas sensor, which needs high conductivity of TiO_2 [19]. It has been reported that the conductivity of the Al-doped TiO_2 is higher than pure TiO_2 in a temperature ranging from 600 ºC to 900 ºC.

In this study, a novel and simple method to produce Fe/ and Al/TiO_2 was developed. The effect of iron and aluminium on TiO_2 was investigated in terms of various iron and aluminium concentrations. $TiCl_4$ as a novel coagulant was co-flocculated with $FeCl_3$ and $Al_2(SO_4)_3$ as conventional coagulants. This novel method produced Fe/TiO_2 and Al/TiO_2. Fe/TiO_2 and Al/TiO_2 were characterized in terms of structural, chemical and photo-electronic properties (X-ray diffraction (XRD), optical absorbance, scanning electron microscopy/energy dispersive X-ray (SEM/EDX) and photocatalytic activity).

Experimental

Organic removal through $TiCl_4$ flocculation in synthetic wastewater

Co-flocculation was carried out with $TiCl_4$ coagulant which was associated with different doses of $FeCl_3$ (0.083 mg/L – 83 mg/L) and $Al_2(SO_4)_3$ (0.038 mg/L – 38 mg/L) in synthetic wastewater. The composition of the synthetic wastewater is presented in Table 1 [20]. This synthetic wastewater represents effluent organic matter generally found in biologically-treated sewage effluent. Tannic acid, peptone, sodium lignin sulfornate, sodium lauryle sulfate and arabic acid represent the larger molecular weight portion, while peptone, beef extract and humic acid comprise the organic matters of lower molecular weight [21]. The samples were stirred rapidly for 1 minute at 100 rpm, followed by 20 minutes of slow mixing at 30 rpm, and 30 minutes of settling. Organic matter was measured using a Dohrmann Phoenix 8000 UV-persulphate TOC analyzer equipped with an autosampler. All samples were filtered through 0.45 µm membrane prior to organic measurement.

Table 1 Constituents of the synthetic wastewater used in this study

Compounds	Concentration (mg/L)	Molecular weight (daltons)	Fraction by organic matter
Beef extract	1.8	300, 100, 70	0.065
Peptone	2.7	34300, 100, 80	0.138
Humic acid	4.2	1500, 300	0.082
Tannic acid	4.2	6300	0.237
Sodium lignin sulfonate	2.4	12100	0.067
Sodium lauryle sulphate	0.94	34300	0.042
Arabic gum powder	4.7	900, 300	0.213
Arabic acid (polysaccharide)	5.0	38900	0.156
$(NH_4)_2SO_4$	7.1		0
K_2HPO_4	7.0		0
NH_4HCO_3	19.8		0
$MgSO_4 \cdot 7H_2O$	0.71		0

Characterization of TiO_2

The visual microscopy was used to measure the shape and aggregated particle size of TiO_2. Scanning electron microscopy/energy dispersive X-ray (SEM/EDX, Rigaku, Japan) was used. XRD images (Rigaku, Japan) of anatase and rutile TiO_2 photocatalysts to identify the particle structure was investigated. All the XRD patterns were analyzed with MDI Jade 5.0 (Materials Data Inc., USA). UV-VIS-NIR spectrophotometer (Cary

500 Scan, Varian, USA) was used to identify the absorbance range and the band gap of TiO_2 was calculated.

The photocatalytic activity test of TiO_2 was investigated under irradiation of UV (Sankyo, F10T8BLB, three 10 W lamps) and visible light (Kumbo, FL10D, three 10W lamps) using the method of photodecomposition of gaseous acetaldehyde. The concentration of acetaldehyde was measured by gas chromatography (Youngin, M600D, Korea).

RESULTS AND DISCUSSION

Dissolved Organic Carbon removal by $TiCl_4$ flocculation

Figure 1 shows the removal of dissolved organic carbon (DOC) after $TiCl_4$ flocculation at different $TiCl_4$ concentrations using synthetic wastewater. The concentration of the $TiCl_4$ coagulants was varied from 2.50 to 13.0 Ti-mg/L. The removal of organic matter was approximately 70% at 8.5 Ti-mg/L of the optimum concentration. The comparison of DOC removal in terms of different coagulants such as Fe- and Al-salt coagulants can be found elsewhere [1]. Shon et al. [1] reported that the size of the settled floc after $TiCl_4$ flocculation was 47.5 μm, which led to faster settling.

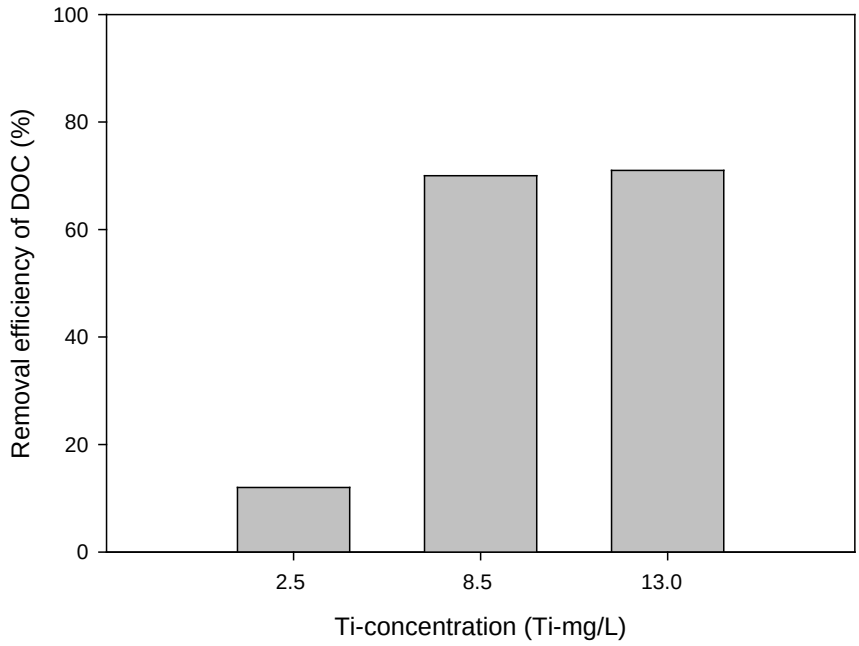

Figure 1 DOC removal by $TiCl_4$ flocculation in synthetic wastewater (initial concentration of DOC = 10.05 mg/L; initial pH = 7.3)

To investigate the effect of co-flocculation by Fe- and Al-salt coagulants with $TiCl_4$ flocculation, $FeCl_3$ and $Al_2(SO_4)_3$ coagulants in the $TiCl_4$ flocculation at the optimum concentration (8.5 Ti-mg/L) in synthetic wastewater were added in the range of 0.083 Fe-mg/L – 83 Fe-mg/L and 0.038 Al-mg/L – 38 Al-mg/L, respectively. The detailed sample information is shown in Table 2. Each sample is named as shown in Table 2 hereafter in this paper.

Table 2 Sample information for the effect of Fe- and Al-salt coagulants with $TiCl_4$ flocculation in synthetic wastewater

Sample name	Concentration of each Fe and Al coagulant added
0.083-Fe/TiO_2	0.083 Fe-mg/L + 8.5 Ti-mg/L flocculation
0.83-Fe/TiO_2	0.83 Fe-mg/L + 8.5 Ti-mg/L flocculation
8.3-Fe/TiO_2	8.3 Fe-mg/L + 8.5 Ti-mg/L flocculation
83-Fe/TiO_2	83 Fe-mg/L + 8.5 Ti-mg/L flocculation
0.038-Al/TiO_2	0.038 Al-mg/L + 8.5 Ti-mg/L flocculation
0.38-Al/TiO_2	0.38 Al-mg/L + 8.5 Ti-mg/L flocculation
3.8-Al/TiO_2	3.8 Al-mg/L + 8.5 Ti-mg/L flocculation
38-Al/TiO_2	38 Al-mg/L + 8.5 Ti-mg/L flocculation

SEM/EDX results

In order to investigate the effect of Fe and Al atoms on TiO_2 produced from the settled floc through Ti-salt flocculation using Fe- and Al-salt coagulants, the settled floc was calcined at 600 ºC. This led to mineralization of all the organic and water compounds. Fe- and Al- doped TiO_2 were prepared and characterized as below.

Figure 2 shows SEM images and EDX spectra of Fe/ and Al/TiO_2 powders at different concentrations of Fe and Al-salts. The samples consisted of particles of various size, shape and dimension. The majority of these particles were found to be less than 1 μm. Further investigations indicated these particles were constituted by agglomerates of a particle (approximately 0.1 μm size). The SEM image of 83-Fe/TiO_2 particles showed

irregular in shape and dimensions compared to other particles. Navio et al. [22] reported that Fe/Ti samples (less than 3 wt% Fe) by a sol-gel method presented deposits irregular in shape and dimensions, while the Fe/Ti samples (more than 5 wt% Fe) showed deposits homogeneous in shape and dimensions. In the case of Al/TiO_2, Lee et al. [18] reported that the size of TiO_2 particles decreased with the increase in Al dopant due to the suppression of particle growth by an introduction of Al atoms into TiO_2 crystal.

EDX analysis was performed to determine the presence of different elements in Fe/ and Al/TiO_2 (Figure 2). Different elements were uniformly spread inside and on the Fe/ and Al/TiO_2 using the EDX mapping technique. The homogeneous distribution of Al and Fe into TiO_2 shows the absence of Al_2O_3 and Fe_2O_3 particles. Fe, Ti, O, C and P were the main constitutive elements of Fe/TiO_2 whereas Al, Ti, O, C and P were in case of Al/TiO_2. The intensity of the Fe element increased with an increase in Fe concentration. However, the intensity of the Al element remained constant with the increase in Al concentration.

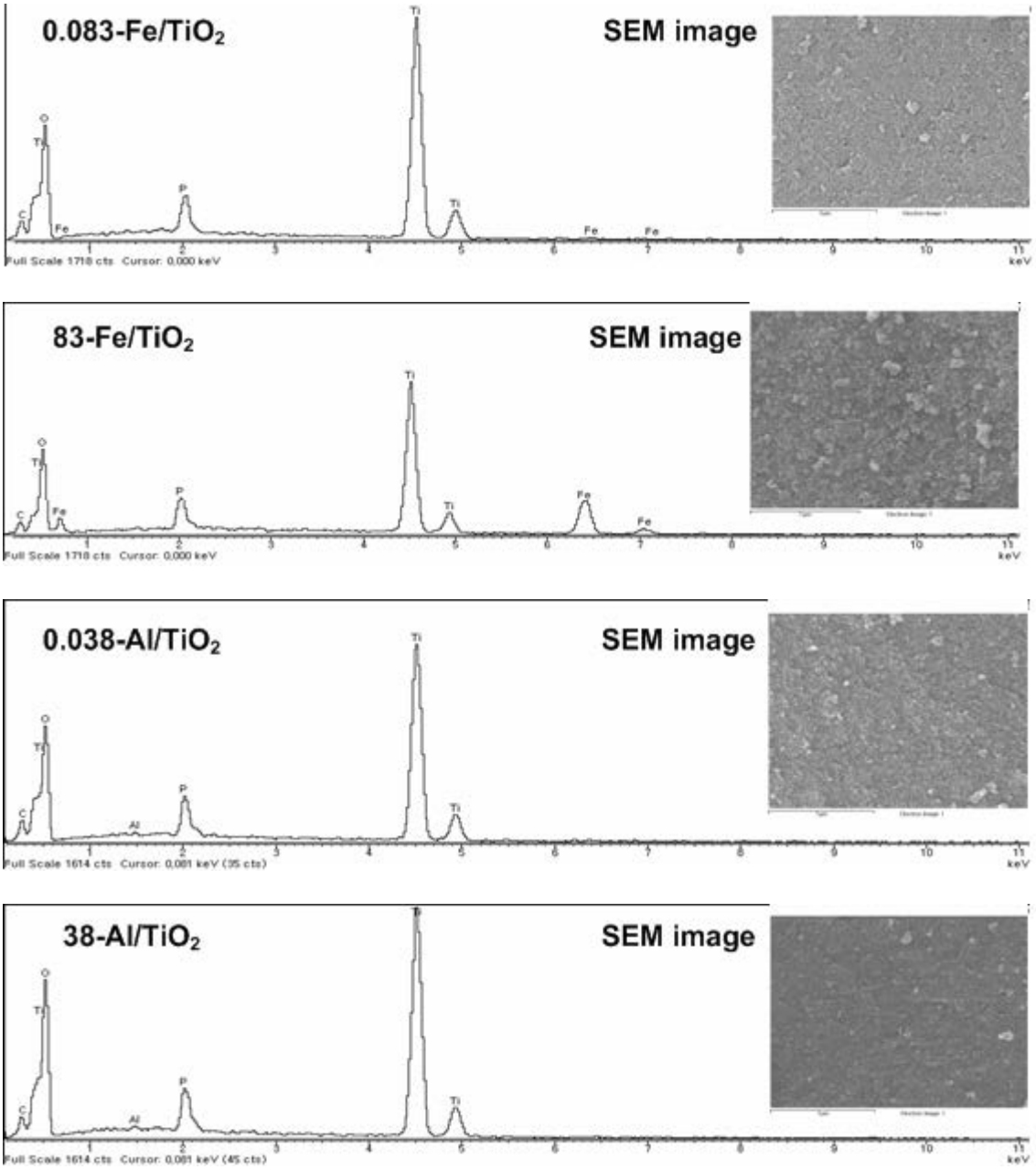

Figure 2 EDX spectra and SEM images of Fe/ and Al/TiO_2 nanoparticles

Tables 3 and 4 show atomic fraction of different elements in Fe/ and Al/TiO_2, respectively. Here, the C atom came from remaining organic carbon of the settled organic matter and phosphorus nutrient present in wastewater was the source of P atom. It is widely accepted that flocculation removes the majority of organic matter and phosphorus [23]. Various trace elements (Si, Fe, Al, V, Ca, Na, Cr, Cl, S, Ni and Br)

were found in TiO_2 retrieved from flocculation sludge. Shon et al. [1] reported that most of the C and P atoms were doped as a substitute site for an O atom, while the Fe and Al atoms would be doped as a substitute site for a Ti atom [24]. As Fe concentration increased, the atomic percentage of the Fe element in Fe/TiO_2 increased significantly from 0.27% (0.083-Fe/Ti) TiO_2 to 9.83% (83-Fe/TiO_2). However, the atomic percentage of the Al element in Al/TiO_2 slightly increased from 0.1% (0.038-Al/TiO_2) to 0.46% (38-Al/TiO_2) with an increase in Al concentration. This indicated that co-flocculation of $FeCl_3$ and $Al_2(SO_4)_3$ with $TiCl_4$ was more favorable with the $FeCl_3$ coagulant than with the $Al_2(SO_4)_3$. Figure 3 shows the linear regression of Fe and Al atomic fraction inside and on TiO_2 versus different Fe and Al concentrations in wastewater. The results suggest that Fe salt flocculation with Ti salt is more favorable to the settled floc.

Table 3 Atomic (%) fraction of Fe/TiO_2 powder at 600 °C calcination with ±3.5% of standard deviation (atomic percentage of P25 TiO_2: Ti = 23.02% and O = 76.98%)

Element	0.083-Fe/Ti TiO_2	0.83-Fe/Ti TiO_2	8.3-Fe/Ti TiO_2	83-Fe/Ti TiO_2
Ti atomic (%)	22.4	20.13	19.66	20.52
C atomic (%)	7.99	8.0	7.84	7.91
P atomic (%)	2.04	3.2	1.88	2.67
O atomic (%)	67.3	68.1	68.7	59.07
Fe atomic (%)	0.27	0.6	1.89	9.83

* Trace elements found: Si (0.2%), S (0.01%), Al (0.01%), V, Ca, Na, Cr, Cl, Ni, and Br

Table 4 Atomic (%) fraction of Al/TiO_2 powder at 600 °C calcination with ±3.5% of standard deviation (atomic percentage of P25 TiO_2: Ti = 23.02% and O = 76.98%)

Element	0.038-Al/Ti TiO_2	0.38-Al/Ti TiO_2	3.8-Al/Ti TiO_2	38-Al/Ti TiO_2
Ti atomic (%)	18.9	21.0	19.87	23.74
C atomic (%)	7.02	9.37	6.86	6.74
P atomic (%)	2.38	2.29	1.93	2.72
O atomic (%)	69.5	67.17	71.14	66.33
Al atomic (%)	0.10	0.16	0.21	0.46

* Trace elements found: Si (0.2%), Fe (0.02%), S (0.01%), V, Ca, Na, Cr, Cl, Ni, and Br

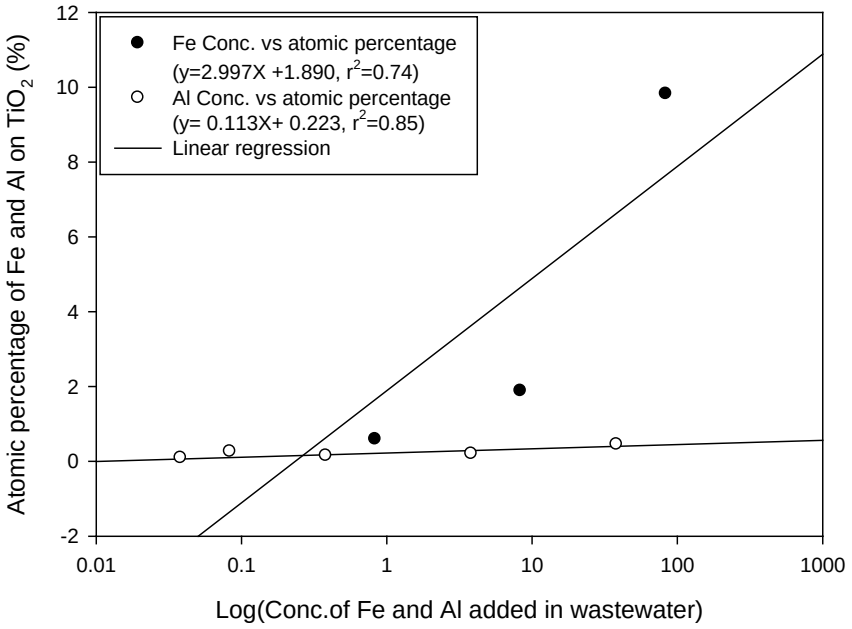

Figure 3 Correlation of concentration of Fe and Al added in synthetic wastewater vs atomic percentage of Fe and Al on/in TiO_2

XRD results

The Fe/ and Al/TiO_2 powder calcined at 600 ºC were investigated in terms of XRD to identify the particle size and structure (Figure 4). The Fe/TiO_2 exhibited the majority of patterns assigned to the anatase phase. At relatively lower iron concentration in TiO_2 (0.083-Fe/TiO_2 – 8.3-Fe/TiO_2), a crystalline phase containing Fe atoms (α-Fe_2O_3, Fe_2TiO_5, etc.) was not observed. This may be due to low concentration of Fe_2O_3 and/or a substitute site (Fe^{3+}) for a Ti^{4+} ion in TiO_2. However, at 83-Fe/TiO_2, hematite (α-Fe_2O_3) was found. This may be due to higher iron concentration. In this study, all the Fe/TiO_2 consisted of the anatase phase. In contrast, Hung et al. [25] reported that the presence of iron may catalyze the transformation of anatase to rutile. The radius of Fe^{3+}

(0.64 Å) is similar to that of Ti^{4+} (0.68 Å). Owing to its smaller size the Fe^{3+} ions present on the surface of TiO_2 iron compact the TiO_2. The iron in the matrix of TiO_2 is a favourable process and easily forms the rutile phase due to open channels. The crystalline size of Fe/TiO_2 at different iron concentrations was investigated by Scherrer's formula [26]. As iron concentration in TiO_2 increased, the anatase phase intensity decreased. This suggests that the Fe species inhibited a crystalline growth (Lee et al., 2004). The crystallite sizes of the Fe/TiO_2 were approximately 11 nm (0.083-Fe/TiO_2) and 5 nm (83-Fe/TiO_2).

XRD analysis of Al/TiO_2 also demonstrates the majority of the anatase phase (Figure 4). A crystalline phase containing Al atoms (α-Al_2O_3, Al_2TiO_5, etc.) was not observed even at higher Al concentrations. This may be due to low concentration of Al_2O_3 and/or a substitute site (Al^{3+}) for a Ti^{4+} ion [27]. Since ionic radius for Al and Ti is also similar (0.68 Å for Al^{3+}), Al can occupy a regular cation position, forming a substitutional solid solution. In addition, Al species dissolved well into the TiO_2 crystal [18]. As discussed above in EDX results, Al/TiO_2 has low atomic percentages in the range from 0.1 at% to 0.46 at% compared with Fe/TiO_2 (from 0.27 at% to 9.83 at%). The crystalline size of Al/TiO_2 at different Al concentrations was investigated by Scherrer's formula. The intensity of the anatase phase decreased with an increase in Al concentration in TiO_2. This suggests that the Al species also inhibited a crystalline growth as did Fe species. The crystallite sizes of the Al/TiO_2 were approximately 11 nm (0.038-Al/TiO_2) and 8 nm (38-Al /TiO_2).

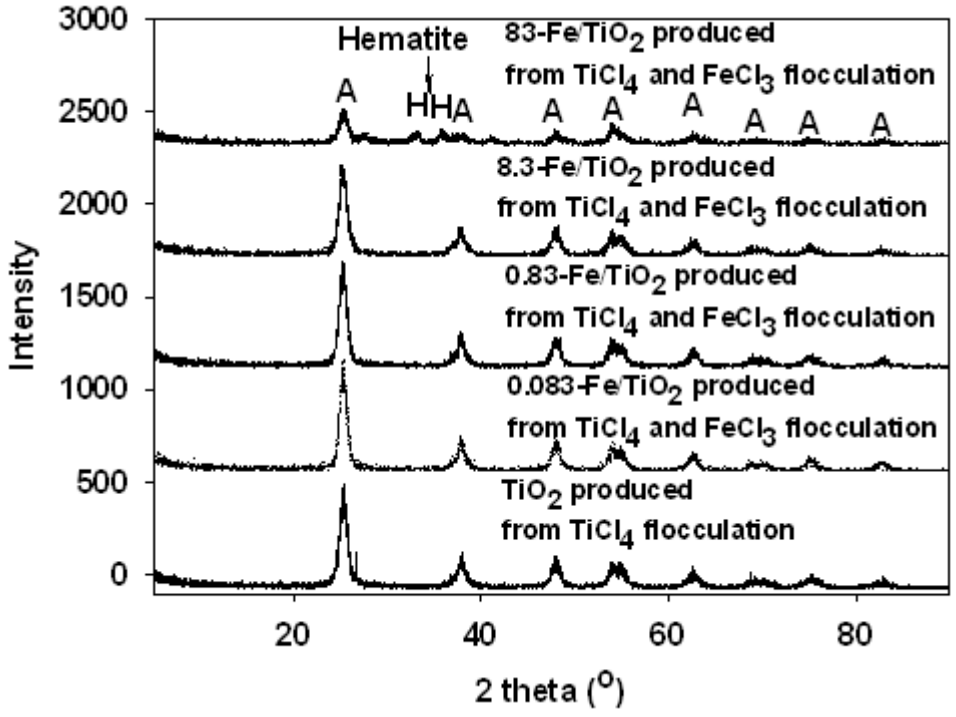

a)

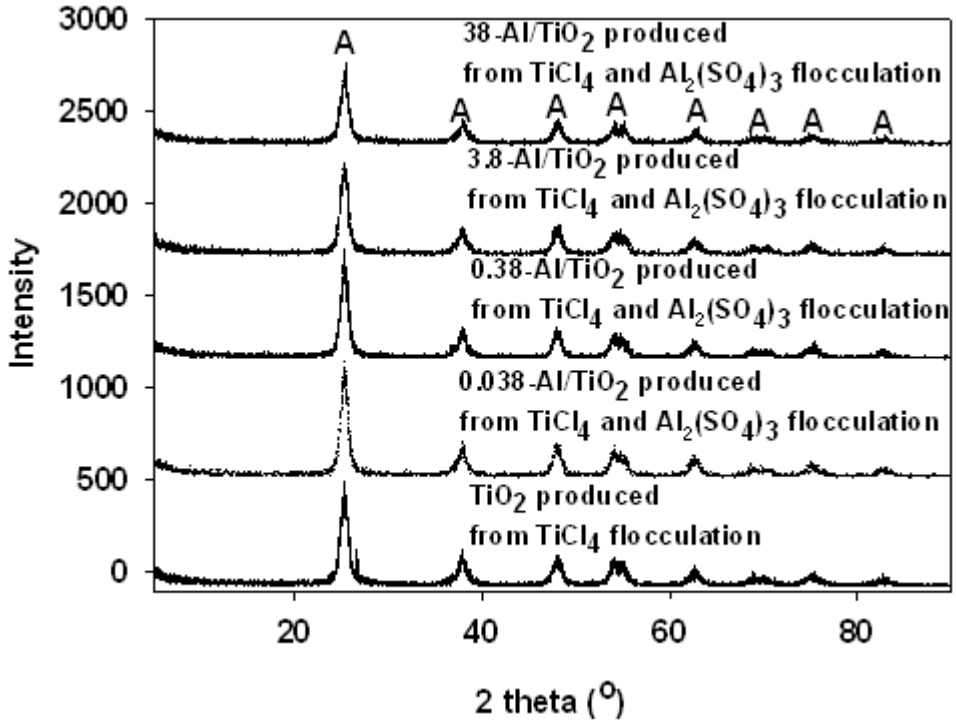

b)

Figure 4 XRD patterns of the Fe and Al-doped TiO_2 particles produced from calcination of the settled floc at 600 ºC a) after $TiCl_4$ and $FeCl_3$ and b) after $TiCl_4$ and $Al_2(SO_4)_3$ flocculation (A: anatase phase (TiO_2); H: hematite (α-Fe_2O_3))

The optical properties of Fe/ and Al/TiO_2 were investigated using the ultra violet–visible-near infrared (UV-VIS-NIR) spectrophotometer (Figure 5). Generally, the absorption band of Ti^{4+} tetrahydral symmetry appears around 300 nm. The absorption bands from 8.3-Fe/TiO_2 concentration of iron ions were shifted significantly up to 500 nm of wavelength. Hung et al. [25] reported that the optimum doping amount of iron ions was 0.005 mol%. UV-Vis diffuse reflectance spectra of Fe/TiO_2 showed an increase in absorbency in the visible light region with the increase in iron ions doping concentration. It was evident that the UV-Vis spectra exhibited an increase in absorbency in the visible light region with an increase in Fe concentration. The red shift associated with the presence of Fe ions may be attributed to: i) a charge transfer transition between the Fe ion electrons and the TiO_2 conduction or valence band and/or ii) a dark reddish colour with the increase of Fe concentration [28]. Al/TiO_2 at different Al concentrations absorbed the majority of UV light (less than 400 nm wavelength). Lee et al. [17] also found that Al/TiO_2 by a sol-gel method mainly absorbed UV light in the range of 1 wt% Al – 10 wt% Al. In contrast, when Al/TiO_2 was prepared using a thermal plasma method, the band edge of the powder shifted from UV region to visible light, suggesting that the shift of absorption spectrum should be attributed to the band gap narrowing relating to the interstitial Al species in the TiO_2 crystal [18].

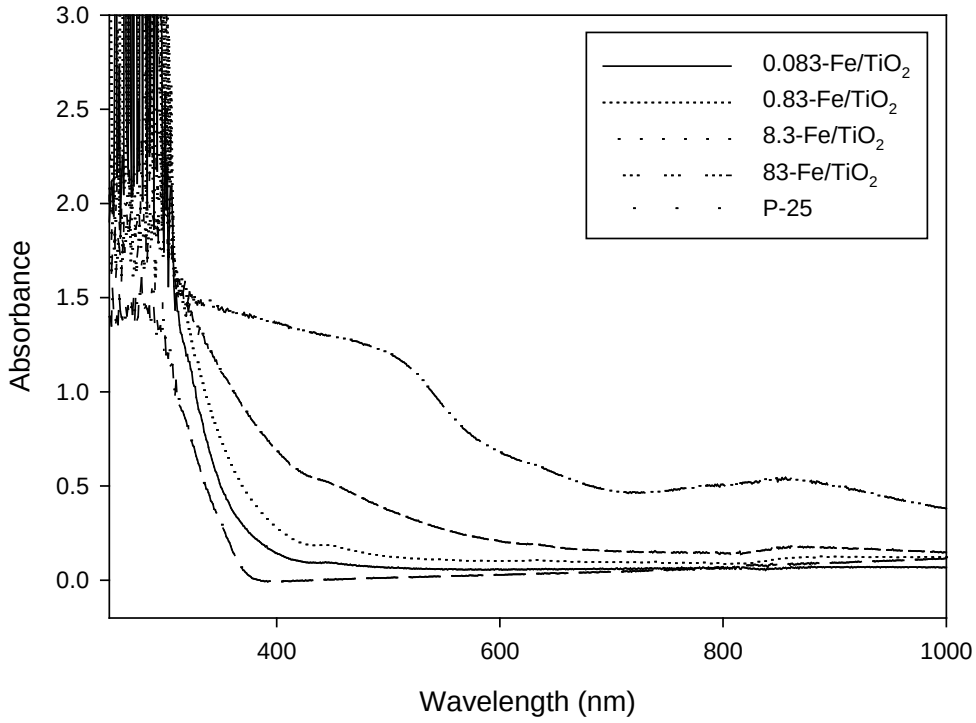

a)

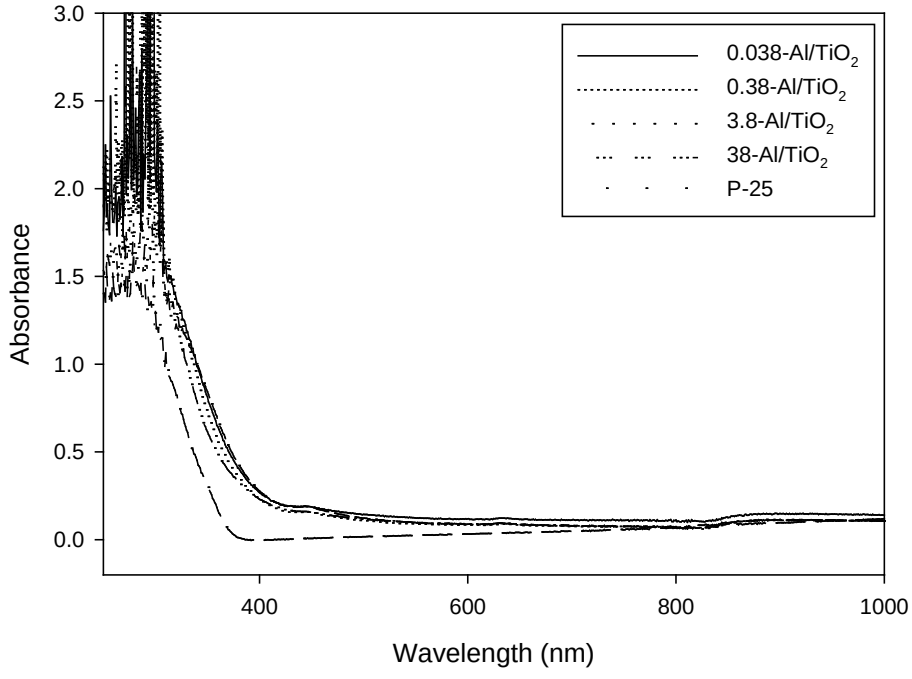

b)

Figure 5 Optical absorbance of a) Fe/TiO_2 and b) Al/TiO_2 at different concentrations of Fe and Al ions

The photo-catalytic property of Fe/ and Al/TiO_2 was examined under irradiation of UV and visible light for the photodecomposition of gaseous acetaldehyde. The concentration of acetaldehyde was measured by gas chromatography. The major portion of acetaldehyde with Fe/ and Al/TiO_2 was significantly removed under UV irradiation within 60 minutes. The low aluminium concentration Al/TiO_2 led to high photoactivity. However, at high iron concentration (8.3 and 83-Fe/TiO_2), acetaldehyde removal by photo-activity under UV irradiation was nominal. This may be due to high iron concentration. Wang et al. [29] reported that formation of Fe_2O_3 and Fe_2TiO_5 at higher calcination temperature (600 ºC - 800 ºC) resulted in a decrease of photo-catalytic activity. Hung et al. [25] reported that the optimum concentration of iron ions was 0.005% (Fe/Ti) and this enhanced gaseous dichloromethane removal. When the concentration of iron ions was high, the iron ions became recombination centers for the electron-hole pairs and reduced the photo-catalytic activity. Under visible light, the photo-decomposition of acetaldehyde using the Fe/ and Al/TiO_2 was marginal.

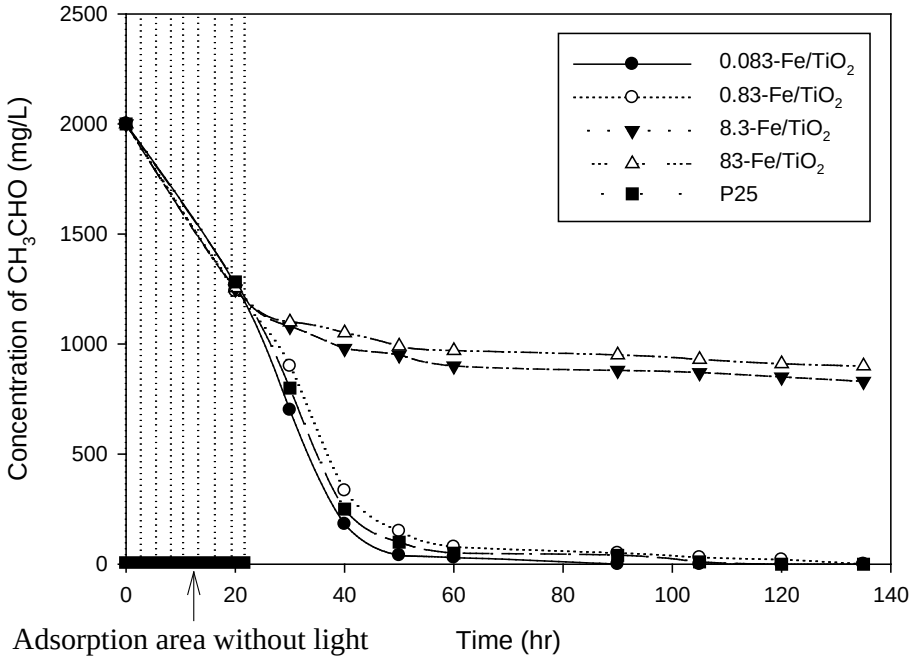

a)

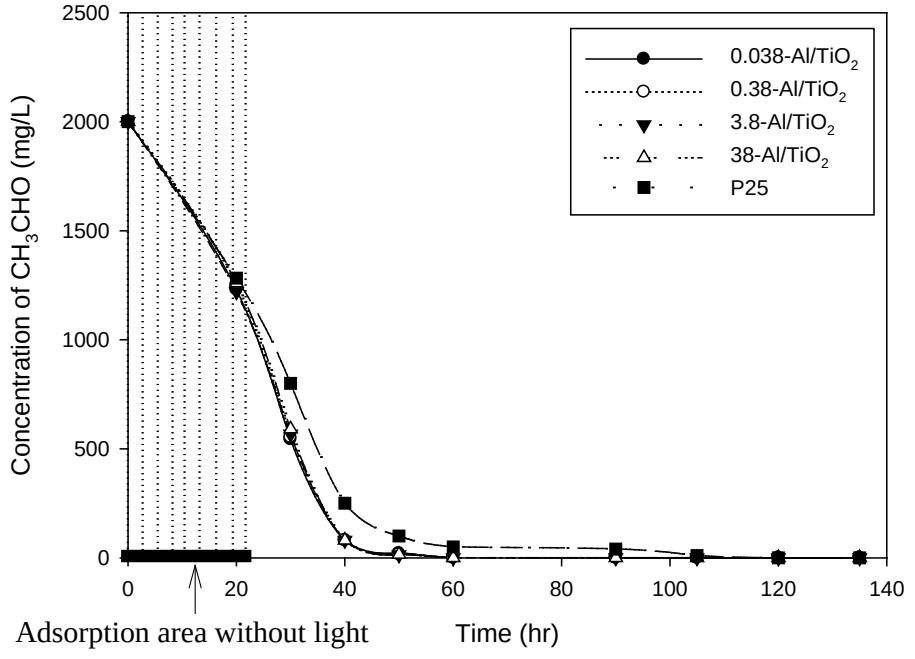

b)

Figure 6 Variation of CH_3CHO concentration with UV irradiation time (initial concentration of CH_3CHO = 2000 mg/L; UV irradiation = black light three 10 W lamps)

CONCLUSIONS

The effect of iron and aluminium on TiO_2 prepared from waste sludge produced by titanium tetrachloride ($TiCl_4$) flocculation of wastewater was investigated in terms of DOC removal, SEM/EDX, XRD, optical absorbance and photocatalytic activity. The results led to the following conclusions:

1. The removal of organic matter by $TiCl_4$ flocculation was approximately 70% at 8.5 Ti-mg/L of the optimum concentration.

2. From SEM observation, the majority of Fe/ and Al/TiO_2 particles were found to be less than 1 μm.

3. From EDX results, main elements of Fe/TiO_2 were Ti, O, C, P and Fe and those of Al/TiO_2 were Ti, O, C, P and Al. The sources of C and P atoms were remaining organic carbon from the settled organic matter and nutrient present in wastewater respectively.

4. As iron concentration increased, the atomic percentage of the Fe element in Fe/TiO_2 increased significantly from 0.27 at% (0.083-Fe/Ti) TiO_2 to 9.83 at% (83-Fe/Ti TiO_2). However, as aluminium concentration increased, the atomic percentage of the Al element in $AlTiO_2$ increased slightly from 0.1 at% (0.038-Al/Ti TiO_2) to 0.46 at% (38-Al/Ti TiO_2). This implied that the $FeCl_3$ is more favourable coagulant than the $Al_2(SO_4)_3$ for co-flocculation with $TiCl_4$.

5. The Fe/TiO_2 exhibited majority of the anatase phase. At low iron concentration in TiO_2 (0.083-Fe/TiO_2 – 8.3-Fe/TiO_2), a crystalline phase containing iron atoms (α- Fe_2O_3, Fe2TiO5, etc.) was not observed. However, at 83-Fe/TiO_2, hematite (Fe_2O_3) was found.

6. The Al/TiO_2 exhibited the anatase phase only at various aluminium concentrations. A crystalline phase containing Al atoms (α-Al_2O_3, Al_2TiO_5, etc.) was not observed even at higher Al concentration. This may be due to the low concentration of Al_2O_3.

7. UV-Vis diffuse reflectance spectra of Fe-TiO_2 show an increase in absorbency in the visible light region with the increase in iron ions doping concentration. Al/TiO_2 at different Al concentrations absorbed the majority of UV light (less than a 400 nm wavelength).

8. The majority of acetaldehyde with Fe/ and Al/TiO_2 was significantly removed under UV irradiation within 60 minutes. Every Al/TiO_2 led to high photoactivity. However, at high iron concentration (8.3 and 83-Fe/TiO_2), acetaldehyde removal by photoactivity under UV irradiation was very low. This may be due to high iron concentration. Under visible light, the photo-decomposition of acetaldehyde using the Fe/ and Al/TiO_2 was marginal.

ACKNOWLEDGMENT

This study was financially supported by Chonnam National University and UTS research grants.

REFERENCES

[1] H.K. Shon, S. Vigneswaran, In S. Kim, J. Cho, G.J. Kim, J-.B. Kim and J-.H. Kim, *Environ. Sci. Technol.* 41, 1372 (2007).

[2] B.Jelks, *Titanium: its occurrence, chemistry and technology*, Ronald Press, New York, 1966, P. 65.

[3] N. Serpone and E. Pelizzetti, *Photocatalysis: fundamentals and applications*, John Wiley & Sons, New York, 1989, p. 125.

[4] M. Kaneko and I. Okura, *Photocatalysis: Science and Technology*, Springer, Tokyo, 2002, p. 84.

[5] D.H. Kim, K.S. Lee, Y.S. Kim, Y.C. Chung and S.J. Kim, *J. Am. Ceram. Soc.*, 89, 515 (2006).

[6] D. Madare, M. Tasca, M. Delibas and G.I. Rusu, *Appl. Surf. Sci.*, 156, 200 (2000).

[7] M.M. Rahman, K.M. Krishna, T. Soga, T. Jimbo and M. Umeno, *J. Phys. Chem. Solids*, 60, 201 (1999).

[8] K.M. Krishna, M. Mosaddeq-ur-Rahman, T. Miki, K.M. Krishna, T. Soga, K. Igarashi, S. Tanemura and M. Umeno, *App. Surf. Sci.*, 113, 149 (1997).

[9] U. Diebold, *Surf. Sci. Rep.*, 48, 53 (2003).

[10] S. Karvinen, *Solid State Sci.*, 5, 811 (2003).

[11] J. Liu, Z. Zheng, K. Zuo and Y. Wu, Preparation and Characterization of Fe3+-doped Nanometer TiO2 Photocatalysts. *Journal of Wuhan University of Technology* (Materials Science Edition), 21, 57 (2006).

[12] W.Y. Teoh, R. Amal, L. Madler and S. E. Pratsinis, *Catal. Today*, 120, 203 (2007).

[13] E. Piera, M.I. Tejedor-Tejedor, M.E. Zorn and M.A. Anderson, *Appl. Catal. B-Enviro.*, 46, 671 (2003).

[14] M.I. Litter, *Appl. Catal. B-Enviro.*, 23, 89 (1999).

[15] D. Chatterjee and S. Dasgupta, *J. Photoch. Photobio. C*, 6, 186 (2005).

[16] C. Li, L. Shi, D. Xie and H. Du, *J. Non-Cryst. Solids*, 352, 4128 (2006).

[17] B.Y. Lee, S.H. Park, M. Kang, S.C. Lee and S.J. Choung, *Appl. Catal. A*, 253, 371 (2003).

[18] J.E. Lee, S.M. Oh and D.W. Park, *Thin Solid Films*, 457, 230 (2004).

[19] Y.J. Choi, Z. Seeley, A. Bandyopadhyay, S. Bose and S.A. Akbar, *Sensor Actuat B-Chem*., In press (2007).

[20] G.T. Seo, S. Ohgaki and Y. Suzuki, *Wat. Sci. Technol.*, 35, 163 (1997).

[21] H.K. Shon, S. Vigneswaran, H.H. Ngo and R. Ben Aim, *Water Res.*, 39, 147 (2005).

[22] J.A. Navio, G. Colon, M. Macias, C. Real and M.I. Litter, *App. Catal. A*, 177, 111 (1999).

[23] H.K. Shon, S. Vigneswaran and S.A. Snyder, *Crit. Rev. Env. Sci. Tec.*, 36, 327 (2006).

[24] H. Yamashita, M. Takeuchi and M. Anpo, *Visible-light-sensitive photocatlaysts*, Encyclopedia of Nanoscience and Nanotechnology, (2004).

[25] W.C. Hung, S.H. Fu, J.J. Tseng, H. Chu and T.H. Ko, *Chemosphere*, 66, 2142 (2007).

[26] Suryanarayana C., *Int. Mater. Rev.*, 40, 41 (1995).

[27] M. Kang, *Mater. Lett.*, 59, 3122 (2005).

[28] J. Zhu, W. Zheng, B. Hea, J. Zhang and M. Anpo, *J. Mol. Catal. A*, 216, 35 (2004).

[29] Z.M. Wang, G. Yang, P. Biswas, W. Bresser and P. Boolchand, *Powder Technol.*, 114, 197 (2001).